CRYSTAL GROWTH & DESIGN

Communication

pubs.acs.org/crystal

Spray Sonocrystallization

Hyo Na Kim, John R. G. Sander, Brad W. Zeiger, and Kenneth S. Suslick*

Department of Chemistry, University of Illinois at Urbana−Champaign, 600 South Mathews Avenue, Urbana, Illinois 61801, United States

Supporting Information

ABSTRACT: A spray sonocrystallization (SSC) method is described here for the crystallization of pharmaceutical agents that provides for a tunable crystal size and narrow size distribution in the submicron regime. SSC uses a tapped, flow-through ultrasonic horn (20 kHz) to spray very fine droplets of the solute-containing solution into a continuous flow of antisolvent which induces immediate crystallization with extremely effective mixing. The analgesic 2-carboxyphenyl salicylate (CPS, salsalate) was explored as a test case. The diameter of sonocrystallized CPS could be controlled systematically over the range from 75 to 175 nm. The addition of low concentrations of polyvinylpyrrolidone or sodium dodecyl sulfate to the antisolvent maintained dispersion of the particles without significantly changing particle size or distribution.

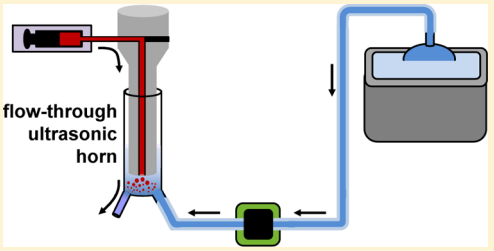

Controlling crystal size and size distribution is crucial in the pharmaceutical industry due to the effects of size on dissolution rates and bioavailability.[1−5] For orally ingested drugs, pharmaceutical agents (PAs), once dissolved, must have sufficient lipophilicity to move across cell membranes but sufficient hydrophilicity to be transported within the body.[6−8] For moderately hydrophobic PAs, however, rates of dissolution after ingestion can be problematic unless the PA crystal size is sufficiently small.[9,10] Aerosol drugs also require control of the particle size and size distribution to successfully administer dosage: particles too large will not get into the deep lung; particles too small will be less easily trapped but more easily absorbed.[11] Parenteral (injected) drugs must also control particle size because potentially fatal embolisms can result with particles larger than ∼5 μm.[12]

In this study, we have coupled intense ultrasound with an antisolvent crystallization method in a continuous flow reactor equipped with a specially designed flow-through ultrasonic horn (Figure 1). The horn has a channel drilled down its center and the PA−solvent solution flows through that channel and is atomized upon its exit from the horn into a flowing stream of antisolvent. The momentum transfer and micromixing created by acoustic cavitation[13−15] forms a fine dispersion of the PA−solvent into the flowing antisolvent, which substantially increases the rate of solvent−antisolvent mixing and leads to rapid formation of nanocrystals at the 100 nm scale. As shown in Figure 2, thorough mixing of solvent and antisolvent occurs within 100 ms.

The analgesic 2-carboxyphenyl salicylate (CPS) was selected as a model system. The solubility of CPS was determined at room temperature in various solvents (Table S1); for example, CPS has high solubility in ethanol (ca. 349 mg/mL), but is poorly soluble in water (<0.01 mg/mL). Based on solubility differences, ethanol and water were chosen as the solvent and antisolvent, respectively. The solvent and antisolvent were

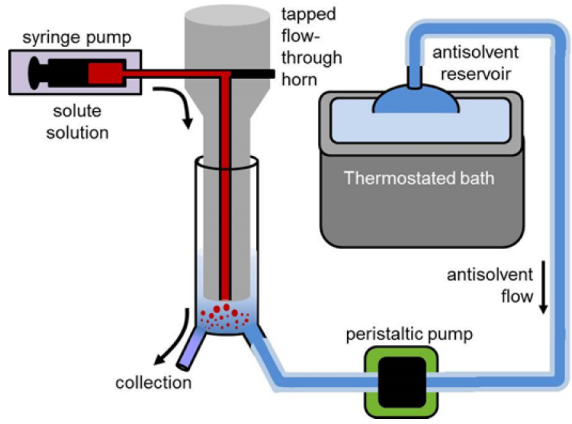

Figure 1. Tapped flow-through ultrasonic horn and experimental rig for spray sonocrystallization.

Figure 2. Mixing pattern of solution (red, flowing from the tapped ultrasonic horn) and antisolvent (white, flowing from the lower right) within the spray sonocrystallization rig. The second frame marks the start of sonication. Frames were extracted from video every 33 ms.

mixed ultrasonically with a mixing ratio of water to CPS solution of 600:1. Thermal equilibration occurred rapidly (<1

Received: January 15, 2015
Revised: March 6, 2015

DOI: 10.1021/acs.cgd.5b00072
Cryst. Growth Des. XXXX, XXX, XXX−XXX

Table 1. Average Crystal Size and Zeta Potential of Sonocrystallized CPS from DLS Measurement

	surfactant concentration, wt %				
	no surfactant	PVP 0.001	PVP 0.01	SDS 0.001	SDS 0.01
Crystal Size, nm	91 ± 5	106 ± 4	99 ± 7	121 ± 9	127 ± 4
Zeta Potential, mV	−37 ± 6	−13 ± 2	−18 ± 2	−60 ± 4	−76 ± 9

min) after energizing the ultrasonic horn (~7 °C rise); unless otherwise specified the reaction zone temperature was 25 °C.

Particle size measurements were made by dynamic light scattering (DLS) measurements (cf. SI experimental section) after 6 min, by which time a crystal size steady state was fully realized (Figure S1). Table 1 gives crystal sizes and zeta potentials of spray sonocrystallized CPS: in the absence of surfactants, the average crystal diameter is 91 ± 5 nm with 96% of crystals falling between ca. 60 and 190 nm (Figure S2). The zeta potential of sonocrystallized CPS is −37 ± 6 mV, which is considered in the moderate stability range (±30 to ± 40 mV).[16] Repeating CPS crystallization in the same cell with the same flow in the absence of ultrasound, but with mechanical mixing (900 rpm, magnetic stir bar), failed to yield product measurable by DLS due to formation of large crystals and aggregation (> ~100 μm) (Figure S3c and Figure S4c,d). In addition, when sonocrystallization of CPS was performed in the presence of an antisolvent but without flow, the product was no longer dispersed nanoparticles, but heavily agglomerated CPS of micron size (Figure S3d and Figure S4e,f).

The sonocrystallized CPS crystals in solution are well dispersed, but after centrifugation or evaporation agglomeration occurs; the agglomerates consist of ca. 100 nm crystals, which match the average crystal diameter value from solution DLS measurements (Figure S4a,b). Despite the agglomeration of the sonocrystallized CPS, there is a clear size reduction of the crystals compared to crystallizations that employ the same flow but with mechanical stirring instead of ultrasound. Mechanically stirred flow crystallization produces ~10-μm-sized crystals that are heavily aggregated (Figures S4c,d and S5). CPS crystals that were generated in the presence of ultrasound but in the absence of antisolvent flow were ~5 μm size, so crystal size reduction was only achieved when sonocrystallization was performed in the flow system (Figures S4e,f and S6).

The addition of surfactants was examined to improve the redispersion of CPS nanocrystals during their isolation (e.g., by centrifugation or evaporation); specifically, either a nonionic (polyvinylpyrrolidone, PVP) or anionic surfactant (sodium dodecyl sulfate, SDS) was added to the antisolvent before spray sonocrystallization. Crystal size was only mildly affected by the surfactant addition (Table 1, Figures S9−10). Powder X-ray diffraction established good crystallinity in sonocrystallized CPS, CPS-PVP, and CPS-SDS nanocrystals, as well as crystals from mechanical stirring (Figures S11−12, Table S2−S3). The surface charge (i.e., zeta potential) of sonocrystallized CPS is affected by the addition of surfactants, as expected. Addition of PVP diminishes the surface charge of the CPS-PVP nanocrystals since PVP increases the thickness of the diffuse double layer.[16] As expected, addition of SDS significantly increases the zeta potential of the CPS-SDS crystals, placing them in the excellent stability range (> ±40),[17] and reduces the expected likelihood of aggregation.

PVP is often used as a dispersant for colloidal solutions and works as a sterically bulky coating of nanoparticles to prevent aggregation. SDS, on the other hand, has a strong negative charge in aqueous solutions and it can prevent aggregation by providing a surface charge upon adsorption to nanoparticle surfaces. Indeed, both surfactants work well to preserve the dispersion of the sonocrystallized nanoparticles. The sonocrystallized CPS-PVP nanocrystals are well-dispersed due to the steric bulk of the PVP substituents (Figure 3a,b and Figure S7a), whereas SDS is effective at minimizing agglomeration of CPS crystals (Figure 3c,d and Figure S7b,c), due to the anionic nature of SDS and the resulting more negative zeta potential of CPS-SDS nanocrystals. Addition of PVP or SDS to solutions that undergo CPS crystallization via mechanical stirring, however, still yielded massively agglomerated product (Figure 3e,f and Figure S7d,e,f). In the absence of antisolvent flow, sonocrystallized CPS are not dispersed and yield an agglomerated product (Figure S8) even in the presence of PVP or SDS.

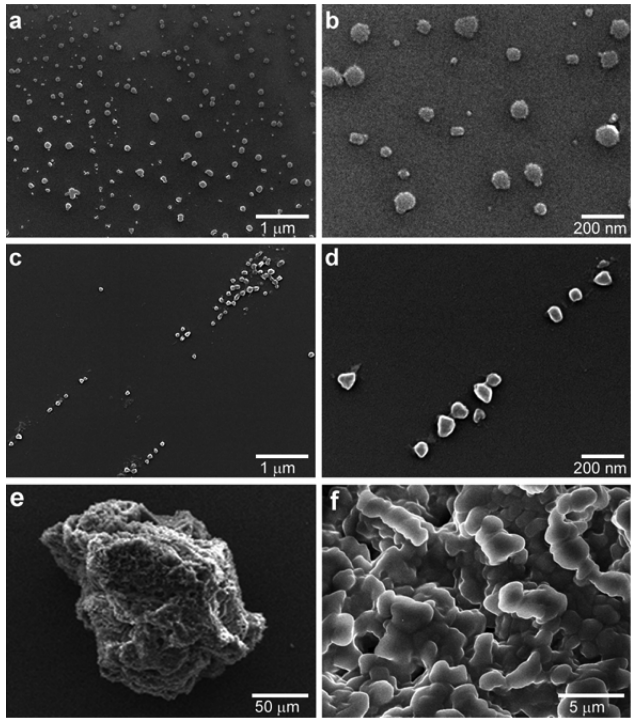

Figure 3. (a,b) SEMs of sonocrystallized CPS with 0.01 wt % PVP added to the antisolvent. (c,d) SEMs of sonocrystallized CPS with 0.01 wt % SDS added. (e,f) SEMs of mechanically stirred (900 rpm) crystallization of CPS with 0.01 wt % PVP added.

In our spray sonocrystallization method, there are various parameters that might affect the sonocrystallization process, including ultrasonic power, flow rate of both antisolvent and solute solution, and concentration of pharmaceutical agent. We have found that the spray sonocrystallization process is robust to most of these variables: the only parameter that has a significant effect on nanocrystal size is the initial solute concentration. Based on DLS measurements, there were no significant changes to average crystal size when ultrasonic power and flow rate were systematically changed (Tables S4

DOI: 10.1021/acs.cgd.5b00072
Cryst. Growth Des. XXXX, XXX, XXX−XXX

and S5). Similarly, the use of different solvents gave rise to only modest changes in the average crystal size. In contrast, however, as the concentration of CPS was increased in the acetone solute solution, the average crystal size also increased (with water as the antisolvent), as shown in Figure 4 and Table S6.

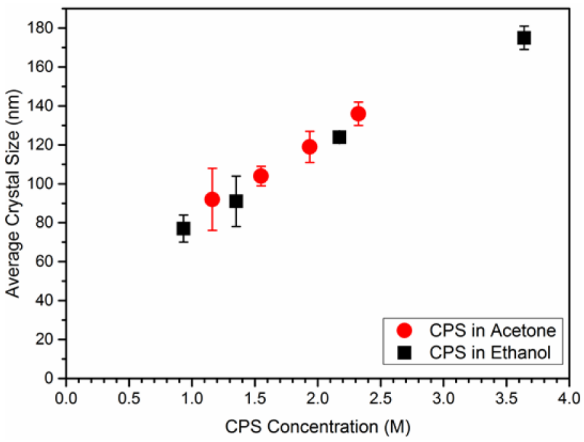

Figure 4. Effect of initial CPS concentration on sonocrystallized CPS size. For acetone, all experiments were at 25 °C; for ethanol, solutions were saturated and crystallizations run at different initial temperatures ranging from 7 to 46 °C.

The CPS concentration was also modified via temperature changes using saturated solutions initially over the range of 7 to 46 °C. As temperature increases, the solubility of CPS increases exponentially (Figure S13), and the average crystal size also increases (Figure 4, Table S7). Based on the results of sonocrystallized CPS in acetone and ethanol with various concentrations, it can be concluded that the higher concentration of CPS produces larger crystals (Figure 4), with an accessible nanocrystal size range of 80 to 180 nm, in this system.

For pharmaceutical agents, a significant problem can be the conversion of metastable crystallites to other morphologies. For this reason, we examined the powder X-ray diffraction (PXRD) of sonocrystallized CPS over a period of several months. CPS crystals, which were generated without or with a surfactant, were centrifuged and dried in a vacuum oven at room temperature immediately after sonocrystallization. They were then stored at room temperature in air as a dried powder and the powder X-ray diffraction was measured periodically: no changes in the PXRD were observed over a 10 month period (Figure S14).

The application of ultrasound during crystallization (i.e., "sonocrystallization") has emerged as an effective means to reduce crystal size and maintain a narrow size distribution. When ultrasound is applied to a liquid, acoustic cavitation occurs: bubbles are formed in the liquid, oscillate and expand, and under certain conditions, implosively collapse.[13−15] Bubble collapse generates intense local heating (~5000 K), pressures (~10^5 kPa), and rapid heating and cooling rates (>10^{10} K/s).[15,18−20] Acoustic cavitation and associated physical consequences of ultrasonic irradiation of liquids increase the number of crystals produced and decreases their size by increasing the rates of both primary and secondary nucleation of crystal growth.

The rates of primary nucleation of embryonic crystallites are increased by ultrasonic irradiation of liquids through three mechanisms: (1) Improved microscale mixing occurs from cavitation and associated turbulence, which accelerates diffusion rates of reactants, thus reducing induction times for crystallization.[21−24] Reduced induction time will increase the rate of nucleation by increasing the growth rates of embryonic crystallites, which prevents their redissolution.[25] (2) Through similar phenomena, ultrasound also reduces the metastable zone width (MZW, i.e., the range of metastability of a supersaturated solution in either temperature or antisolvent concentration[25]), which diminishes the rate of crystal growth and decreases crystal size.[23,26−28] (3) The increase in gas−liquid interfaces produced by bubble formation, collapse, and fragmentation can also enhance nucleation rates.[25]

Rates of secondary nucleation are also increased by ultrasonic irradiation. Breakage of primary crystals due to interparticle collisions or more importantly shockwave fragmentation during sonication (i.e., "sonofragmentation")[29,30] increases the number of secondary nucleation sites, which results in increased numbers of smaller crystals. Turbulent flow from cavitation will also diminish crystal aggregation, which produces smaller solid particulates with narrower size distribution.

Antisolvent crystallization (i.e., adding a miscible liquid in which the solute is poorly soluble) can generate a high level of supersaturation quickly and induce higher nucleation rates.[4,25,31−34] In principle, ultrasound should be beneficial for antisolvent crystallization through enhanced mixing between the antisolvent and solution; in practice, however, the ultrasound from a solid horn has been applied to the merging of fairly wide streams (25 mm) of solvent and antisolvent or to a large volume batch reactor of antisolvent into which the solute solution is pumped; these configurations lead to ineffective application of the ultrasound with relatively poor mixing and generation of multimicron-sized crystals.[35−40]

In conclusion, the spray sonocrystallization method produces nanoscaled pharmaceutical molecular crystals with a narrow size distribution. Nanocrystal size can be easily controlled through solute concentration. Nonionic and anionic surfactants, PVP and SDS, effectively reduce aggregation of the nanocrystals. Given the lower ultrasonic power demands necessary for these laboratory scale experiments, we have some confidence that one may achieve scale-up to kg levels without great difficulty.

■ ASSOCIATED CONTENT

Supporting Information

Experimental procedures, sample characterization, solubility tests, steady state check, particle size distributions, optical micrographs, SEM images, powder X-ray diffraction data, and DLS results about variation of parameters. This material is available free of charge via the Internet at http://pubs.acs.org.

■ AUTHOR INFORMATION

Corresponding Author

*E-mail: ksuslick@illinois.edu. Tel: 217-333-2794. Fax: 217-244-3186.

Notes

The authors declare no competing financial interest.

■ ACKNOWLEDGMENTS

This research was supported by NSF DMR 1206355. This work was carried out in part in the Frederick Seitz Materials Research Laboratory Central Facilities, UIUC.

DOI: 10.1021/acs.cgd.5b00072
Cryst. Growth Des. XXXX, XXX, XXX−XXX

REFERENCES

(1) Erdemir, D.; Lee, A. Y.; Myerson, A. S. Nucleation of crystals from solution: classical and two-step models. *Acc. Chem. Res.* **2009**, *42* (5), 621−629.

(2) Chen, J.; Sarma, B.; Evans, J. M.; Myerson, A. S. Pharmaceutical crystallization. *Cryst. Growth Des.* **2011**, *11* (4), 887−895.

(3) Duncan, R.; Gaspar, R. Nanomedicine (s) under the microscope. *Mol. Pharmaceutics* **2011**, *8* (6), 2101−2141.

(4) D'Addio, S. M.; Prud'homme, R. K. Controlling drug nanoparticle formation by rapid precipitation. *Adv. Drug Delivery Rev.* **2011**, *63* (6), 417−426.

(5) Abu Bakar, M. R.; Nagy, Z. K.; Saleemi, A. N.; Rielly, C. D. The impact of direct nucleation control on crystal size distribution in pharmaceutical crystallization processes. *Cryst. Growth Des.* **2009**, *9* (3), 1378−1384.

(6) Liversidge, G. G.; Cundy, K. C. Particle size reduction for improvement of oral bioavailability of hydrophobic drugs: I. Absolute oral bioavailability of nanocrystalline danazol in beagle dogs. *Int. J. Pharm.* **1995**, *125* (1), 91−97.

(7) Amidon, G. L.; Lennernäs, H.; Shah, V. P.; Crison, J. R. A theoretical basis for a biopharmaceutic drug classification: the correlation of in vitro drug product dissolution and in vivo bioavailability. *Pharm. Res.* **1995**, *12* (3), 413−420.

(8) Balaz, S. Modeling kinetics of subcellular disposition of chemicals. *Chem. Rev.* **2009**, *109* (5), 1793−1899.

(9) Kesisoglou, F.; Panmai, S.; Wu, Y. Nanosizing—oral formulation development and biopharmaceutical evaluation. *Adv. Drug Delivery Rev.* **2007**, *59* (7), 631−644.

(10) Sun, W.; Mao, S.; Shi, Y.; Li, L. C.; Fang, L. Nanonization of itraconazole by high pressure homogenization: stabilizer optimization and effect of particle size on oral absorption. *J. Pharm. Sci.* **2011**, *100* (8), 3365−3373.

(11) Kleinstreuer, C.; Zhang, Z.; Donohue, J. Targeted drug-aerosol delivery in the human respiratory system. *Annu. Rev. Biomed. Eng.* **2008**, *10*, 195−220.

(12) Devadasu, V. R.; Bhardwaj, V.; Kumar, M. R. Can controversial nanotechnology promise drug delivery? *Chem. Rev.* **2012**, *113* (3), 1686−1735.

(13) Leighton, T. *The Acoustic Bubble*; Academic Press: London, 1994.

(14) Suslick, K. S. Sonochemistry. *Science* **1990**, *247* (4949), 1439−1445.

(15) Suslick, K. S.; Flannigan, D. J. Inside a collapsing bubble: sonoluminescence and the conditions during cavitation. *Annu. Rev. Phys. Chem.* **2008**, *59*, 659−683.

(16) Verma, S.; Gokhale, R.; Burgess, D. J. A comparative study of top-down and bottom-up approaches for the preparation of micro/nanosuspensions. *Int. J. Pharm.* **2009**, *380* (1), 216−222.

(17) Greenwood, R.; Kendall, K. Selection of suitable dispersants for aqueous suspensions of zirconia and titania powders using acousto-phoresis. *J. Eur. Ceram. Soc.* **1999**, *19* (4), 479−488.

(18) McNamara, W. B.; Didenko, Y. T.; Suslick, K. S. Sonoluminescence temperatures during multi-bubble cavitation. *Nature* **1999**, *401* (6755), 772−775.

(19) Flannigan, D. J.; Suslick, K. S. Plasma formation and temperature measurement during single-bubble cavitation. *Nature* **2005**, *434* (7029), 52−55.

(20) McNamara, W. B.; Didenko, Y. T.; Suslick, K. S. Pressure during sonoluminescence. *J. Phys. Chem. B* **2003**, *107* (30), 7303−7306.

(21) Guo, Z.; Zhang, M.; Li, H.; Wang, J.; Kougoulos, E. Effect of ultrasound on anti-solvent crystallization process. *J. Cryst. Growth* **2005**, *273* (3), 555−563.

(22) Lyczko, N.; Espitalier, F.; Louisnard, O.; Schwartzentruber, J. Effect of ultrasound on the induction time and the metastable zone widths of potassium sulphate. *Chem.—Eng. J.* **2002**, *86* (3), 233−241.

(23) Revalor, E.; Hammadi, Z.; Astier, J.-P.; Grossier, R.; Garcia, E.; Hoff, C.; Furuta, K.; Okustu, T.; Morin, R.; Veesler, S. Usual and unusual crystallization from solution. *J. Cryst. Growth* **2010**, *312* (7), 939−946.

(24) Guo, Z.; Jones, A.; Li, N. The effect of ultrasound on the homogeneous nucleation of BaSO4 during reactive crystallization. *Chem. Eng. Sci.* **2006**, *61* (5), 1617−1626.

(25) Mullin, J. W. *Crystallization*; Butterworth-Heinemann: Oxford, 2001.

(26) Cravotto, G.; Gaudino, E. C.; Cintas, P. On the mechanochemical activation by ultrasound. *Chem. Soc. Rev.* **2013**, *42* (18), 7521−7534.

(27) Li, H.; Li, H.; Guo, Z.; Liu, Y. The application of power ultrasound to reaction crystallization. *Ultrason. Sonochem.* **2006**, *13* (4), 359−363.

(28) Luque de Castro, M.; Priego-Capote, F. Ultrasound-assisted crystallization (sonocrystallization). *Ultrason. Sonochem.* **2007**, *14* (6), 717−724.

(29) Zeiger, B. W.; Suslick, K. S. Sonofragmentation of molecular crystals. *J. Am. Chem. Soc.* **2011**, *133* (37), 14530−14533.

(30) Sander, J. R.; Zeiger, B. W.; Suslick, K. S. Sonocrystallization and sonofragmentation. *Ultrason. Sonochem.* **2014**, *21* (6), 1908−1915.

(31) Dirksen, J.; Ring, T. Fundamentals of crystallization: kinetic effects on particle size distributions and morphology. *Chem. Eng. Sci.* **1991**, *46* (10), 2389−2427.

(32) Kamaraju, V. K.; Chiu, M.-S. Improved operation of concentration control for antisolvent crystallization processes. *Org. Process Res. Dev.* **2015**, *19*, 178−188.

(33) Myerson, A. *Handbook of Industrial Crystallization*; Butterworth-Heinemann: Oxford, 2002.

(34) Thorat, A. A.; Dalvi, S. V. Liquid antisolvent precipitation and stabilization of nanoparticles of poorly water soluble drugs in aqueous suspensions: Recent developments and future perspective. *Chem. Eng. J.* **2012**, *181*, 1−34.

(35) Eder, R. J.; Schrank, S.; Besenhard, M. O.; Roblegg, E.; Gruber-Woelfler, H.; Khinast, J. G. Continuous sonocrystallization of acetylsalicylic acid (ASA): control of crystal size. *Cryst. Growth Des.* **2012**, *12* (10), 4733−4738.

(36) Beck, C.; Dalvi, S. V.; Dave, R. N. Controlled liquid antisolvent precipitation using a rapid mixing device. *Chem. Eng. Sci.* **2010**, *65* (21), 5669−5675.

(37) Dalvi, S. V.; Dave, R. N. Controlling particle size of a poorly water-soluble drug using ultrasound and stabilizers in antisolvent precipitation. *Ind. Eng. Chem. Res.* **2009**, *48* (16), 7581−7593.

(38) Narducci, O.; Jones, A.; Kougoulos, E. An assessment of the use of ultrasound in the particle engineering of micrometer-scale adipic acid crystals. *Cryst. Growth Des.* **2011**, *11* (5), 1742−1749.

(39) Ramisetty, K. A.; Pandit, A. B.; Gogate, P. R. Ultrasound-assisted antisolvent crystallization of benzoic acid: effect of process variables supported by theoretical simulations. *Ind. Eng. Chem. Res.* **2013**, *52* (49), 17573−17582.

(40) Sander, J. R.; Bučar, D. K.; Henry, R. F.; Zhang, G. G.; MacGillivray, L. R. Pharmaceutical nano-cocrystals: sonochemical synthesis by solvent selection and use of a surfactant. *Angew. Chem.* **2010**, *122* (40), 7442−7446.

DOI: 10.1021/acs.cgd.5b00072
Cryst. Growth Des. XXXX, XXX, XXX−XXX